

DiffVSR: Enhancing Real-World Video Super-Resolution with Diffusion Models for Advanced Visual Quality and Temporal Consistency

Xiaohui Li^{1,2*} Yihao Liu^{2,*†} Shuo Cao^{3,2} Ziyang Chen⁴ Shaobin Zhuang¹
 Xiangyu Chen² Yinan He² Yi Wang² Yu Qiao^{2,4}

¹Shanghai Jiao Tong University ²Shanghai Artificial Intelligence Laboratory ³University of Science and Technology of China

⁴Shenzhen Institute of Advanced Technology, Chinese Academy of Sciences

<https://xh9998.github.io/DiffVSR-project/>

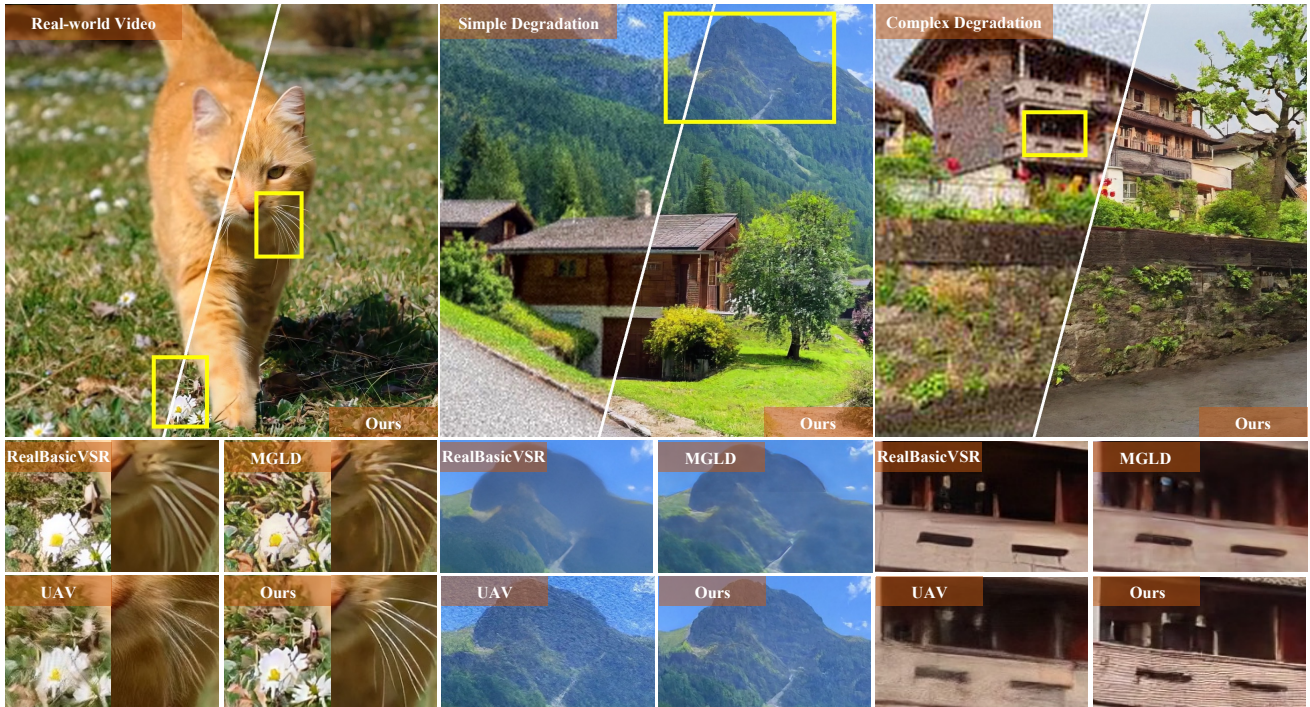


Figure 1. Restoration results on real-world and synthetic (simple/complex degradation) videos. Our DiffVSR shows consistent effectiveness across diverse degradation scenarios. (Zoom in for best view)

Abstract

Diffusion models have demonstrated exceptional capabilities in image generation and restoration, yet their application to video super-resolution faces significant challenges in maintaining both high fidelity and temporal consistency. We present DiffVSR, a diffusion-based framework for real-world video super-resolution that effectively addresses these challenges through key innovations. For intra-sequence coherence, we develop a multi-scale temporal attention module and temporal-enhanced VAE de-

coder that capture fine-grained motion details. To ensure inter-sequence stability, we introduce a noise rescheduling mechanism with an interweaved latent transition approach, which enhances temporal consistency without additional training overhead. We propose a progressive learning strategy that transitions from simple to complex degradations, enabling robust optimization despite limited high-quality video data. Extensive experiments demonstrate that DiffVSR delivers superior results in both visual quality and temporal consistency, setting a new performance standard in real-world video super-resolution.

*Equal contribution. †Corresponding author.

1. Introduction

With the widespread use of video capture and storage devices, the digital video industry has rapidly expanded across media platforms such as television, streaming networks, and mobile applications. To continuously enrich the human visual experience, real-world video super-resolution (VSR) has emerged as a critical research area in both academia and industry. The goal of real-world VSR is to reconstruct high-resolution (HR) video frames from their low-resolution (LR) counterparts, which often suffer from noise, blur, compression artifacts, and other complex degradations. The primary challenge lies in achieving high-quality results that balance excellent visual quality with satisfactory temporal consistency – a difficult trade-off highlighted in numerous studies [6, 42].

Traditional VSR approaches, typically based on convolutional neural networks (CNNs) [6, 42] or recurrent structures [8, 23], are effective at maintaining temporal consistency but often fail to generate fine-grained textures and realistic details. Recently, diffusion models [14, 32] have shown remarkable success in high-quality image generation and restoration tasks, offering a promising approach to overcome these limitations. However, the stochastic nature of diffusion models tends to introduce severe temporal flickering artifacts, which are highly detrimental to the viewing experience. Despite recent efforts [3] to improve temporal consistency using additional temporal layers, these models still produce videos with reduced sharpness and temporal jitter, due to limited high-quality video data and the complexity of optimizing both spatial and temporal dimensions.

To address these challenges, we identify two primary issues for diffusion-based VSR methods. First, maintaining both intra-sequence and inter-sequence temporal consistency is crucial for achieving smooth, coherent transitions within and across video sequences. Second, more effective and robust optimization strategies are essential to enhance visual quality and fully leverage the generative prior’s potential for realistic, high-fidelity video reconstruction. In response to these challenges, we propose DiffVSR, a diffusion-based real-world video super-resolution model that achieves advanced visual quality without sacrificing temporal consistency, as illustrated in Fig. 2.

Intra-sequence Temporal Consistency. When processing long videos, it is common to segment them into sub-sequences (*e.g.*, each with 8 frames) and apply the VSR model to each sub-sequence independently before stitching the results. Temporal consistency within each sub-sequence can be improved by incorporating 3D convolutional layers and temporal attention mechanisms. To further enhance intra-sequence coherence, we introduce a multi-scale temporal attention (MSTA) module that captures diverse motion and texture details through multi-scale information fusion, as shown in Fig. 2(b). Additionally, we investigate var-

ious Variational Autoencoder (VAE) variants and propose a temporal-enhanced VAE to improve consistency.

Inter-sequence Temporal Consistency. The stochasticity of diffusion models often leads to abrupt transitions between sequences. We observe that the temporal consistency in video diffusion models is strongly coupled with both the input video content and the initial diffusion sampling noise [32]. Previous approaches have utilized optical flow guidance [6] to achieve global consistency by aligning and fusing frames; however, this method relies heavily on optical flow accuracy and adds computational overhead. As noted by Chan *et al.* [9], long-term information propagation can amplify artifacts in real-world VSR due to error accumulation. To address this, we adopt a noise rescheduling mechanism combined with an interweaved latent transition (ILT) approach to enhance inter-sequence consistency, as detailed in Fig. 3. This post-processing solution avoids additional modules or retraining, providing an efficient method to improve coherence across sequences.

Optimization Strategy. Effective learning strategies are essential for training video diffusion models, especially when high-quality video data is scarce — a challenge that is currently under-explored. Previous methods [3] often train the model directly on complex degradations, fine-tuning only the parameters of the added temporal layers. Our findings indicate that a phased training strategy not only increases training efficiency but also enhances stability and overall performance. Initially, we fix the parameters of the pretrained text-to-image (T2I) base model [32] and train a foundational VSR model on a large, lower-quality dataset with simple degradations, as directly learning complex degradations can be challenging. In the second stage, we introduce progressively complex degradations to refine this baseline model. Finally, we fine-tune the model on high-quality data, fully unfreezing all parameters to enable precise adaptation to real-world conditions. This gradual transition from simple to complex data, combined with selective parameter optimization, ensures robust learning and maximizes model stability and generalization across varied degradations.

In summary, by deeply investigating the crucial factors of diffusion-based VSR methods, we propose DiffVSR, a practical solution that achieves both high visual quality and temporal consistency. We introduce a multi-scale temporal attention module and a temporal-enhanced VAE decoder to improve intra-sequence consistency. For inter-sequence consistency, we implement a noise rescheduling mechanism combined with an interweaved latent transition approach. Additionally, we design a progressive learning strategy to stabilize training and enhance the model’s capability to handle various degradations. Extensive experiments have demonstrated that DiffVSR outperforms existing methods in both visual quality and temporal consistency, establishing

a new state-of-the-art in real-world video super-resolution.

2. Related Work

Single image super-resolution (SISR) aims at recovering a high-resolution (HR) image from its low-resolution (LR) counterpart. Recent years have seen SISR methods achieved significant success by leveraging powerful generative prior. With degradation models widely explored and models specifically crafted, GAN-based methods [10, 22, 41, 43, 50] has achieved photo-realistic results. With the development and prosperity of diffusion models and communities, diffusion-based methods [11, 25, 38, 47] further elevate the SISR performance to a new level due to its stable large-scale training.

Intuitively, **video super-resolution (VSR)** can be systematically viewed as an extension of SISR by processing inputs of LR image sequences. Beyond this basic extension, a typical VSR method further takes advantage of the additional inter-sequence information to enhance performance. Previous VSR methods tend to introduce sophisticated model structure to incorporate the temporal information [16, 26, 44], such as optical flow estimation along with feature alignment and fusion [5, 6, 24]. TDAN [36] and EDVR [42] further introduce deformable convolution to achieve better feature alignment [7]. The recurrent structure is additionally designed for multi-frame output [6, 8, 23, 27]. These designs are usually effective for maintaining temporal consistency but struggle to yield high-quality details.

However, the above-mentioned blessing of additional temporal information can turn into a curse when introducing generative prior into VSR methods. The inherent randomness of each recovered frame from generative models tends to bring sequence jitter, which introduces new challenges for maintaining both inter-sequence and intra-sequence temporal consistency [22]. Few attempts have been made to alleviate this negative effect. Upscale-A-Video [53] employs additional temporal layers and recurrent latent propagation. Mainly designed for enhancing contents of text-to-video generation, VEnhancer [12] achieves flexible space and time upsampling by leveraging a video controlnet [51]. MGLD [48] crafts optical-flow module as motion guidance into diffusion sampling process.

3. Method

Real-world video super-resolution (VSR) poses challenges in handling complex degradations, generating high-quality textures, and maintaining temporal consistency – issues that are especially difficult for diffusion-based methods due to the stochastic nature of the diffusion process.

To address these challenges, our DiffVSR model integrates key components that enhance both visual qual-

ity and temporal consistency, as depicted in Fig. 2. Given degraded video input, we first leverage InternLM-XComposer2 [35] to automatically provide descriptive text annotations that capture high-fidelity visual details and semantic information. These text prompts effectively activate the model’s capability in generating fine-grained textures during the restoration process. For intra-sequence consistency, we introduce a multi-scale temporal attention module and a temporal-enhanced VAE. For inter-sequence consistency, we propose an interweaved latent transition approach with noise rescheduling mechanism. Additionally, a staged learning strategy is employed to stabilize training and improve efficiency. These targeted improvements significantly boost the model performance, providing a practical recipe for adapting diffusion models to real-world VSR task.

3.1. Preliminary: Generative Diffusion Prior

Our model is built upon the pretrained large-scale text-to-image latent diffusion model (LDM), Stable Diffusion x4 Upscaler [1]. It first pretrains an autoencoder that converts an image x into a low-dimensional latent z with an encoder \mathcal{E} , and reconstructs it with a decoder \mathcal{D} . The core of this framework is a conditional denoising U-Net that operates in the compressed latent space.

During training, given a latent sample $z \sim p_{data}$, Gaussian noise is added following a predefined schedule to generate noisy latents $z_t = \alpha_t z + \sigma_t \epsilon$, where $\epsilon \sim \mathcal{N}(0, I)$, and α_t, σ_t define the noise schedule at timestep t . To enhance detail generation, the input low-resolution image x is also perturbed with noise $x_\tau = \alpha_\tau x + \sigma_\tau \epsilon$, where τ corresponds to early diffusion steps. Following v -prediction parameterization [33], the U-Net denoiser f_θ is optimized to predict $v_t \equiv \alpha_t \epsilon - \sigma_t x$ by minimizing:

$$\mathcal{L} = \mathbb{E}_{z,x,c,t,\epsilon} [\|v_t - f_\theta(z_t, x_\tau; c, t)\|_2^2], \quad (1)$$

where c represents conditional inputs including text prompts and noise levels. During inference, the model iteratively denoises the latent representation conditioned on the low-resolution input, with flexible control over the sampling process through text prompts and noise scheduling.

3.2. Multi-Scale Temporal Attention

To address temporal flickering in video diffusion models, existing approaches typically introduce 3D convolution and temporal attention into pretrained image-based SD models. While temporal attention reduces temporal inconsistencies, we observe a trade-off: models that prioritize temporal coherence often generate smoother but less detailed textures, diminishing the visual quality of outputs. To overcome this, we propose a multi-scale temporal attention (MSTA) module that leverages multi-scale information fusion to capture diverse motion and texture details, as shown in Fig. 2(d).

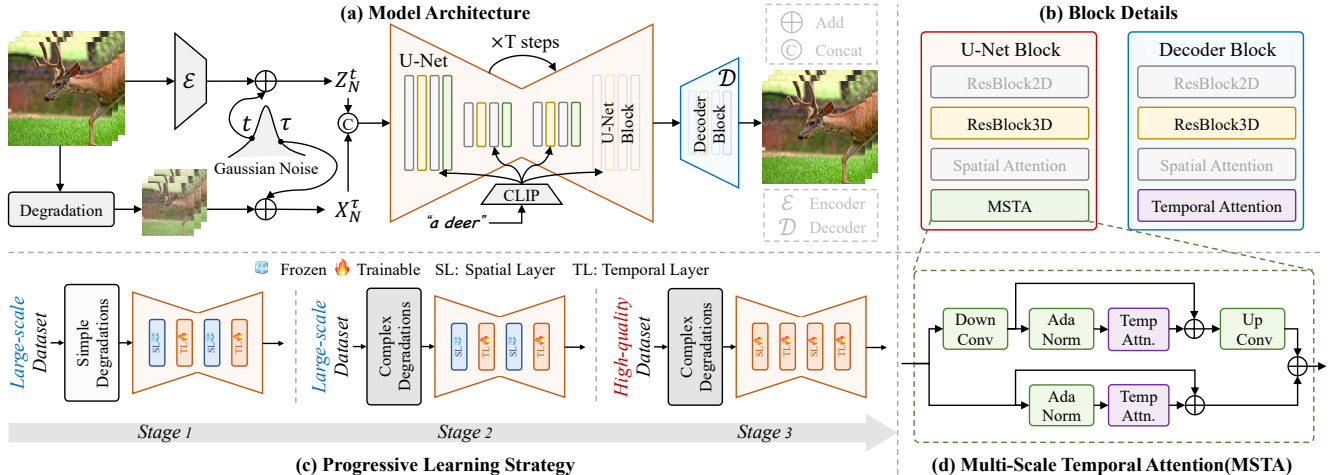


Figure 2. Overview of our proposed DiffVSR framework. (a) The overall model architecture integrates enhanced UNet and VAE decoder for high-quality frame restoration. (b) Detailed designs of our modified UNet and VAE decoder blocks for better feature extraction and reconstruction. (c) Progressive Learning Strategy that enables stable training and robust performance across various degradation levels. (d) Multi-Scale Temporal Attention (MSTA) mechanism designed for capturing temporal dependencies at different scales. Notably, spatial layer includes ResBlock2D and Spatial Attention, while temporal layer contains ResBlock3D, Temporal Attention and MSTA module.

Given an intermediate hidden embedding h in the U-Net, we first downsample it using strided convolution to obtain $h_{\downarrow} = \text{DConv}(h)$. Temporal attention is then applied separately to both h_{\downarrow} and the original h :

$$\begin{aligned} h_{\text{down}} &= \text{TA}(\text{AdaLN}(h_{\downarrow})) + h_{\downarrow}, \\ h_{\text{ori}} &= \text{TA}(\text{AdaLN}(h)) + h, \end{aligned} \quad (2)$$

where TA represents the temporal attention operation and AdaLN denotes adaptive layer normalization. After upsampling h_{down} , we combine it with the original temporal attention branch output to produce the final hidden embedding h' :

$$h' = h_{\text{down}} + \alpha \cdot \text{UPConv}(h_{\text{down}}), \quad (3)$$

where UPConv is the upsampling layer, and α is the fusion weight (set to 0.5). This multi-scale approach enhances the model's capacity to capture varied motion patterns and long-range temporal dependencies, enabling it to balance temporal consistency with fine-grained texture generation.

3.3. Temporal-Enhanced 3DVAE

Ensuring temporal consistency in the denoising U-Net reduces flickering, but improving the U-Net alone is insufficient for stable video output. The Variational Autoencoder (VAE) component also significantly impacts temporal stability, as it directly generates the final results. The original VAE in the SD x4 Upscaler is a 2D model pretrained on static images, which can cause temporal inconsistencies in video frames, particularly in fine-grained regions.

To address this, we examine two extensions to the original 2D VAE. The first variant, 3DVAE, incorporates an additional 3D residual block following the 2D residual block,

enabling the model to capture short-term temporal dependencies. Building on this, the second variant, Temporal-Enhanced 3DVAE (TE-3DVAE), further improves temporal coherence by adding a temporal attention layer after the spatial attention layer, enhancing longer-term temporal modeling across frames.

We train these VAE variants using a combination of L1 reconstruction loss, perceptual loss [52], and adversarial loss with a temporal PatchGAN discriminator [18]. As shown in our ablation studies (Table 4), both variants significantly improve temporal consistency and restoration quality compared to the baseline 2D VAE. In our model, we adopt the TE-3DVAE for its superior performance.

3.4. Interweaved Latent Transition

To efficiently process long video sequences, we segment the entire sequence into multiple overlapping subsequences $\{L_0, L_1, \dots, L_N\}$. After processing each subsequence L_i with the UNet, we obtain a corresponding latent feature sequence list F_i . Due to independent processing, adjacent subsequences may exhibit visual discontinuities. To address this, we propose an Interweaved Latent Transition (ILT) method that blends the latent features in overlapping regions, ensuring smooth transitions across frames, as illustrated in Fig. 3. Unlike previous works [6, 40], the proposed ILT does not rely on flow estimation or additional training. For each pair of consecutive latent sequences F_i and F_{i+1} , ILT linearly interpolates the latents in the overlapping frames. Specifically, for the j -th frame in the overlap region, the fused latent sequence is computed as:

$$F_{\text{fused}}[j] = \alpha_j F_i[s+j] + (1 - \alpha_j) F_{i+1}[j], \quad (4)$$

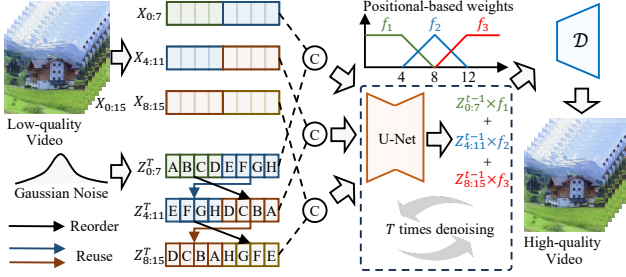


Figure 3. Illustration of our temporal consistency enhancement approach. Noise rescheduling mechanism that reuses and reorders noise frames across overlapping regions. Interweaved Latent Transition (ILT) scheme that performs position-based latent interpolation between adjacent subsequences. This lightweight post-processing solution effectively ensures temporal consistency without additional training or computational overhead.

where $\alpha_j = 1 - \frac{j}{(P-1)}$ is the position-based fusion weight, P is the number of overlapping frames, and s denotes the overlapping window stride. In our implementation, each subsequence contains $N_{test} = 8$ frames with a 4-frame overlap, providing a sufficient buffer for smooth blending while balancing computational efficiency. By interpolating latents based on frame positions, ILT effectively reduces artifacts and minimizes abrupt transitions, ensuring a visually consistent output across the entire sequence.

Noise rescheduling. As noted by [15, 46], temporal consistency in video diffusion models is strongly coupled with both input video content and the initial noise used in diffusion sampling. Inspired by this observation, we incorporate a noise rescheduling mechanism with the ILT process to further enhance frame continuity, as shown in Fig. 3. Specifically, we initialize a set of N_{test} random noise frames $[\epsilon_1, \epsilon_2, \dots, \epsilon_{N_{test}}]$ for the first sequence. For each subsequent subsequence, we iteratively reuse and reorder these noise frames within overlapping regions, ensuring consistent noise across frames. This approach effectively aligns the diffusion process across frames, reducing temporal jitter and improving stability in highly detailed regions.

3.5. Progressive Learning Strategy

Taming a diffusion-based model for real-world VSR requires a carefully structured learning approach to achieve both efficiency and high-quality results. Previous methods often attempt to directly train on data with complex degradations, which result in over-smoothed outputs due to the model’s struggle to simultaneously handle intricate temporal relationships and severe degradations [9, 43]. This is especially problematic given the scarcity of high-quality video data. To address this, we propose a progressive learning strategy that gradually builds the model’s capacity in three stages.

Stage 1: Temporal Layer Fine-tuning. In the first stage, we freeze all spatial layers and focus solely on fine-tuning the temporal layers on large-scale dataset. We introduce only simple degradations (Gaussian blur and bicubic down-sampling) at this stage, which encourages the model to learn smooth transitions over time without the added burden of complex degradation artifacts. This targeted fine-tuning allows the frame-based diffusion model to develop a foundational capability for handling temporal consistency across consecutive frames.

Stage 2: Complex Degradation Adaptation. In the second stage, we introduce complex degradations, including noise, compression artifacts, and other real-world distortions [9, 43]. Building on the temporal consistency established in the first stage, the model is now equipped to learn to adapt to these more challenging degradations. This staged progression from simple to complex degradations enables the model to handle real-world artifacts more effectively.

Stage 3: High-quality Refinement. In the final stage, we fine-tune all layers of the model, using high-quality video data to further refine both spatial and temporal restoration capabilities. Fine-tuning with high-quality data allows the model to learn to generate sharper, more visually appealing results, with refined details and reduced artifacts. This final step is crucial for achieving high realistic textures in restored videos, ensuring that the model not only handles complex degradations but also enhances perceptual quality.

By progressively introducing complexity through this staged learning approach, our model effectively learns to handle increasingly challenging inputs and degradation scenarios in real-world VSR applications. Experimental results demonstrate that this strategy significantly outperforms direct training on complex degradations (see Section 4.3).

4. Experiments

4.1. Datasets and Implementation Details

Datasets. We primarily use WebVid-2M [2], a large-scale dataset containing 2.5M text-video pairs with resolution of 336×596, for stages 1 and 2 training. Stage 3 fine-tuning utilizes OpenVid-1M [31] containing 1M high-resolution (512×512 or larger) text-video pairs and YouHQ [53] containing 37K 2K-resolution videos without text annotations. We employ the degradation pipeline from RealBasicVSR [9] to generate low-quality inputs. For evaluation, we test on both synthetic datasets (REDS4 [30], SPMCS [34], UDM10 [49]), and two variants of YouHQ40 [53] with different degradation levels) and real-world datasets (MVSR4x [39] and our collected RealVideo10 with diverse scenes).

Training Details. We implement our model using PyTorch and train it on 8 NVIDIA A100 GPUs. During training,

Datasets	Metrics	Real-ESRGAN[43]	SD ×4 Upscaler[1]	DiffBIR[25]	RealBasicVSR[9]	MGLD[48]	VEnhancer[12]	UAV[53]	Ours
REDS4	PSNR↑	23.269	21.987	24.116	25.715	24.427	20.500	23.919	23.411
	CLIP-IQA↑	0.640	0.670	0.521	0.673	0.584	0.587	0.553	0.710
	MUSIQ↑	69.384	68.544	69.478	66.990	64.368	49.194	45.708	70.670
	DOVER↑	0.718	0.675	0.665	0.705	0.713	0.677	0.576	0.687
SPMCS	PSNR↑	23.105	21.011	23.261	24.986	24.087	19.613	22.627	23.122
	CLIP-IQA↑	0.796	0.837	0.743	0.802	0.778	0.765	0.773	0.826
	MUSIQ↑	69.762	68.982	70.940	68.327	65.343	59.370	66.273	71.615
	DOVER↑	0.762	0.795	0.759	0.736	0.692	0.696	0.694	0.772
UDM10	PSNR↑	26.872	24.039	26.767	28.526	27.801	23.134	27.412	26.966
	CLIP-IQA↑	0.708	0.775	0.679	0.735	0.695	0.671	0.681	0.736
	MUSIQ↑	61.792	64.689	64.562	64.248	60.470	54.449	56.633	67.731
	DOVER↑	0.815	0.827	0.784	0.814	0.780	0.735	0.723	0.826
YouHQ40	PSNR↑	24.421	21.687	24.154	24.818	24.524	21.230	23.529	23.713
	CLIP-IQA↑	0.766	0.752	0.722	0.797	0.745	0.768	0.708	0.785
	MUSIQ↑	62.050	62.623	67.522	65.398	63.407	52.493	57.141	68.040
	DOVER↑	0.876	0.854	0.840	0.885	0.847	0.814	0.815	0.878
YouHQ40 (complex deg.)	PSNR↑	22.122	21.034	22.347	22.247	22.503	20.908	21.836	22.159
	CLIP-IQA↑	0.715	0.718	0.651	0.745	0.724	0.711	0.659	0.767
	MUSIQ↑	58.866	47.475	65.157	66.471	57.219	39.036	57.469	67.679
	DOVER↑	0.634	0.092	0.624	0.676	0.594	0.225	0.606	0.710
MVSR4x	NRQM↑	4.731	3.081	6.564	5.746	4.665	2.417	5.582	6.432
	CLIP-IQA↑	0.460	0.397	0.407	0.426	0.487	0.468	0.395	0.491
	MUSIQ↑	54.331	22.670	62.599	62.716	50.367	31.109	56.128	66.829
	DOVER↑	0.634	0.092	0.624	0.676	0.594	0.225	0.606	0.710
RealVideo10	NRQM↑	4.495	4.801	6.880	5.680	4.768	3.641	5.399	5.805
	CLIP-IQA↑	0.831	0.846	0.803	0.836	0.861	0.785	0.835	0.856
	MUSIQ↑	49.733	39.920	58.647	61.121	52.332	39.003	50.029	59.566
	DOVER↑	0.704	0.485	0.716	0.773	0.714	0.670	0.610	0.749

Table 1. Quantitative comparison with state-of-the-art methods on synthetic datasets (REDS4, SPMCS, UDM10, YouHQ40) and real-world datasets (MVSR4x, RealVideo10). The best and second-best results are marked in red and blue respectively.

we use AdamW [20] optimizer with learning rate of $1e-4$. The batch size is 96. We randomly crop patches of size 320×320 from training videos with a length of 8 frames to generate LR-HR pairs, where the temporal sampling stride varies from 1 to 6 to capture different motion patterns.

Evaluation Metrics. For quality assessment, we adopt both fidelity-based metric (PSNR) and perceptual-driven metrics (CLIP-IQA [37], MUSIQ [19], NRQM [29], and DOVER [45]). Temporal consistency is measured by warping error (E_{warp}^*) [21], background consistency (BC) [17], and temporal flickering (TF) [17].

4.2. Comparisons

For comprehensive evaluation, we compare our method against state-of-the-art approaches, including both image-based restoration methods (Real-ESRGAN [43], SD ×4 Upscaler [1], DiffBIR [25]) and video restoration methods (RealBasicVSR [9], MGLD [48], VEnhancer [12], UAV [53]).

Quantitative Evaluation. We evaluate our method on seven datasets, including both synthetic degradation datasets and real-world datasets. As shown in Table 1, while traditional methods like RealBasicVSR achieve higher PSNR scores due to their tendency towards over-smoothing, our method demonstrates superior performance in perceptual quality metrics. Specifically, we achieve the best or second-best performance in CLIP-IQA and MUSIQ across most datasets, indicating better restoration of fine details

and textures. On REDS4, our method achieves the highest CLIP-IQA (0.710) and MUSIQ (70.670) scores, significantly outperforming other approaches. Similar results can be observed on other datasets, particularly in challenging scenarios like YouHQ40 with complex degradation, where our method leads in CLIP-IQA (0.767), MUSIQ (67.679), and DOVER (0.710).

Qualitative Evaluation. We present visual comparisons on synthetic datasets in Fig. 12 and real-world datasets in Fig. 11, respectively. For synthetic degradation scenarios, our method demonstrates superior capability in recovering fine-grained details. In Fig. 12, our approach accurately reconstructs the facial hair texture and successfully restores the text on the billboard, while other methods produce either over-smoothed or distorted results.

In real-world scenarios, our method exhibits strong performance in preserving structural details and natural textures. The first row of Fig. 11 shows our method’s effectiveness in maintaining sharp geometric structures and depth information. In the underwater scene, our approach vividly reconstructs the distinctive texture of the sea turtle’s skin, while other methods tend to generate rock-like artificial patterns. More visual results can be found in the supplementary file.

Temporal Consistency. We select representative methods to evaluate temporal consistency. Table 2 suggests that our method maintains competitive temporal consistency while



Figure 4. Qualitative comparisons on synthetic low-quality videos from YouHQ40 and UDM10 datasets. Among the tested methods, only our approach can recover the accurate facial beard texture and produce detailed text on the billboard. **(Zoom-in for best view)**

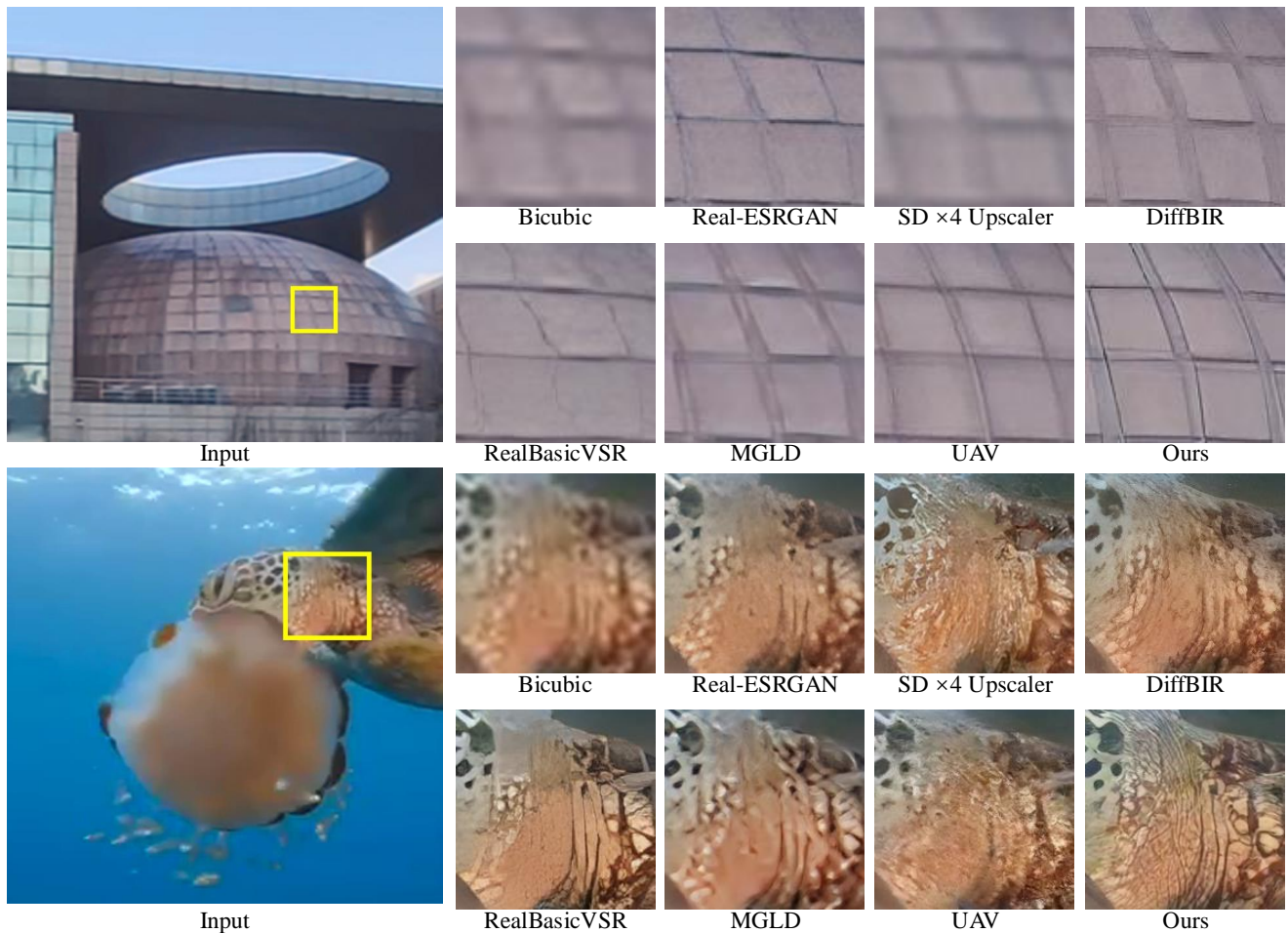


Figure 5. Qualitative comparisons on real-world test videos from MVSR4x and RealVideo10 datasets. Our method effectively leverages the advantages in generating high-quality results. When compared to existing methods, it notably excels in its restoration capabilities, successfully recovering architectural textures and depth details. In particular, our method accurately restores the natural skin texture of sea turtles in underwater scenes, while other methods incorrectly render the turtle’s skin with stone-like textures. **(Zoom-in for best view)**

achieving superior perceptual quality. Notably, on RealVideo10, DiffVSR achieves the highest BC score (0.971)

while maintaining competitive TF performance.

The temporal profile visualization in Fig. 6 provides in-

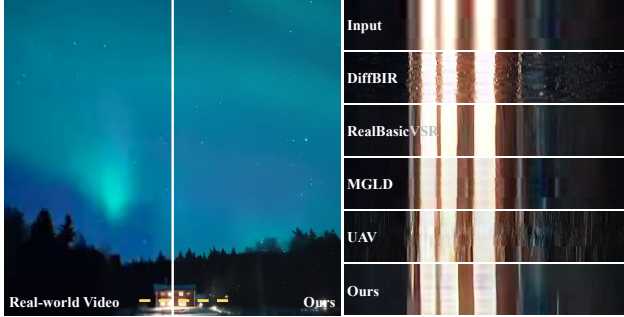


Figure 6. Temporal profiles on a RealVideo10 sequence. By stacking frame scan lines (yellow dashed line) chronologically, we observe that image-based method exhibits temporal flickering, while our approach demonstrates both superior restoration quality and smooth temporal transitions. (Best viewed on digital displays)

Datasets	Metrics	DiffBIR	RealBasicVSR	MGLD	UAV	Ours
SPMCS	$E_{warp}^* \downarrow$	3.503	0.638	0.865	1.266	1.121
	BC \uparrow	0.955	0.976	0.981	0.968	0.972
	TF \uparrow	0.959	0.975	0.981	0.973	0.972
RealVideo10	$E_{warp}^* \downarrow$	1.978	1.204	1.070	0.997	1.321
	BC \uparrow	0.959	0.955	0.969	0.971	0.971
	TF \uparrow	0.958	0.966	0.969	0.968	0.965

Table 2. Quantitative temporal comparison on SPMCS and RealVideo10. BC denotes Background Consistency and TF denotes Temporal Flickering.

tuitive temporal analysis. Single-image methods like DiffBIR exhibit noticeable temporal jitter, manifesting as irregular patterns in the temporal profile (as shown in the second row of Fig. 6). In contrast, our method and other video-based approaches maintain smooth temporal transitions, shown by the consistent patterns in the temporal dimension. This qualitative observation aligns with our quantitative metrics, confirming that our method can well balance high perceptual quality with temporal stability.

Exp.	MSTA	PLS	ILT	PSNR \uparrow	SSIM \uparrow	$E_{warp}^* \downarrow$	TF \uparrow
(a)	✓			23.570	0.601	2.834	0.953
(b)	✓	✓		23.939	0.628	2.056	0.952
(c)	✓	✓	✓	24.172	0.635	1.707	0.955

Table 3. Ablation study on YouHQ10 (subset of YouHQ40) dataset with TE-3DVAE, showing the contribution of each component (MSTA, PLS, and ILT) to the overall performance.

4.3. Ablation Study

We conduct extensive ablation studies to validate the effectiveness of our proposed components: Multi-Scale Temporal Attention (MSTA), Progressive Learning Strategy (PLS), Interweaved Latent Transition (ILT), and Temporal-Enhanced 3DVAE (TE-3DVAE).

Effectiveness of Temporal-Enhanced 3DVAE. We train

	PSNR \uparrow	SSIM \uparrow	$E_{warp}^* \downarrow$	TF \uparrow
2DVAE	30.251	0.917	1.049	0.965
3DVAE	30.645	0.926	0.800	0.967
TE-3DVAE	30.874	0.927	0.761	0.968

Table 4. Quantitative comparison of VAE variants (2DVAE, 3DVAE, and TE-3DVAE) on VAE-VAL5 dataset. The results show that 3D architecture improves over 2D, while temporal enhancement further boosts performance across all metrics.

all VAE variants on OpenVid-1M and evaluate them on our collected VAE-VAL5 dataset for texture and motion assessment. As shown in Table 4, compared to 2D VAE, 3D VAE improves PSNR by 0.4dB and reduces warping error by 24%. Our TE-3DVAE further achieves the best performance in both restoration quality and temporal consistency, demonstrating effective temporal information preservation in the latent space.

Effectiveness of Multi-Scale Temporal Attention. As shown in Table 3, MSTa serves as the foundation of our framework (Exp. a). Even with MSTa alone, our model achieves reasonable performance across all metrics, indicating its effectiveness in capturing temporal dependencies at different scales. It suggests that MSTa can well balance temporal consistency with fine-grained texture generation.

Effectiveness of Progressive Learning Strategy. Adding PLS (Exp. b) significantly improves the model’s performance, with PSNR increasing by 0.37dB and warping error dropping by 27%, demonstrating that PLS helps the model learn more stable temporal representations. Moreover, the introduction of PLS fortifies the model’s ability to handle complex scenes and high-speed motions.

Effectiveness of Interweaved Latent Transition. The full model with ILT (Exp. c) achieves the best performance across all metrics. Compared to Exp. b, incorporating ILT further improves PSNR by 0.23dB and reduces warping error, validating our design choice of interweaving latent transitions for better temporal feature propagation. The progressive improvements from Exp. a to c confirm that each proposed component contributes positively to the overall performance. The combination of all components achieves the best balance between quality and temporal consistency.

5. Conclusion

We present a novel video restoration framework for real-world low-quality video super-resolution that incorporates four key innovations: Temporal-Enhanced 3D VAE for temporal-aware feature encoding, Multi-Scale Temporal Attention for dynamic information capture, Interweaved Latent Transition for long sequence temporal coherence, and Progressive Learning Strategy. Extensive experiments demonstrate our method’s superior performance in both synthetic and real-world scenarios, particularly in recovering fine-grained visual details with competitive temporal

consistency. Our approach achieves state-of-the-art results in perceptual quality and visual fidelity across multiple challenging datasets and comprehensive evaluation metrics, while maintaining long-term temporal stability.

References

- [1] Stability AI. Stable diffusion x4 upscaler. <https://huggingface.co/stabilityai/stable-diffusion-x4-upscaler>, 2022. 3, 6, 14
- [2] Max Bain, Arsha Nagrani, Gül Varol, and Andrew Zisserman. Frozen in time: A joint video and image encoder for end-to-end retrieval. In *Proceedings of the IEEE/CVF international conference on computer vision*, pages 1728–1738, 2021. 5
- [3] Andreas Blattmann, Robin Rombach, Huan Ling, Tim Dockhorn, Seung Wook Kim, Sanja Fidler, and Karsten Kreis. Align your latents: High-resolution video synthesis with latent diffusion models. In *Proceedings of the IEEE/CVF Conference on Computer Vision and Pattern Recognition*, pages 22563–22575, 2023. 2
- [4] Yochai Blau and Tomer Michaeli. The perception-distortion tradeoff. In *Proceedings of the IEEE Conference on Computer Vision and Pattern Recognition (CVPR)*, 2018. 12
- [5] Jiezhong Cao, Yawei Li, Kai Zhang, and Luc Van Gool. Video super-resolution transformer. *arXiv preprint arXiv:2106.06847*, 2021. 3
- [6] Kelvin CK Chan, Xintao Wang, Ke Yu, Chao Dong, and Chen Change Loy. Basicvsr: The search for essential components in video super-resolution and beyond. In *Proceedings of the IEEE/CVF conference on computer vision and pattern recognition*, pages 4947–4956, 2021. 2, 3, 4
- [7] Kelvin CK Chan, Xintao Wang, Ke Yu, Chao Dong, and Chen Change Loy. Understanding deformable alignment in video super-resolution. In *Proceedings of the AAAI conference on artificial intelligence*, pages 973–981, 2021. 3
- [8] Kelvin CK Chan, Shangchen Zhou, Xiangyu Xu, and Chen Change Loy. Basicvsr++: Improving video super-resolution with enhanced propagation and alignment. In *Proceedings of the IEEE/CVF conference on computer vision and pattern recognition*, pages 5972–5981, 2022. 2, 3
- [9] Kelvin CK Chan, Shangchen Zhou, Xiangyu Xu, and Chen Change Loy. Investigating tradeoffs in real-world video super-resolution. In *Proceedings of the IEEE/CVF Conference on Computer Vision and Pattern Recognition*, pages 5962–5971, 2022. 2, 5, 6, 12, 14
- [10] Chaofeng Chen, Xinyu Shi, Yipeng Qin, Xiaoming Li, Xiaoguang Han, Tao Yang, and Shihui Guo. Real-world blind super-resolution via feature matching with implicit high-resolution priors. In *Proceedings of the 30th ACM International Conference on Multimedia*, pages 1329–1338, 2022. 3
- [11] Ben Fei, Zhaoyang Lyu, Liang Pan, Junzhe Zhang, Weidong Yang, Tianyue Luo, Bo Zhang, and Bo Dai. Generative diffusion prior for unified image restoration and enhancement. In *Proceedings of the IEEE/CVF Conference on Computer Vision and Pattern Recognition*, pages 9935–9946, 2023. 3
- [12] Jingwen He, Tianfan Xue, Dongyang Liu, Xinqi Lin, Peng Gao, Dahua Lin, Yu Qiao, Wanli Ouyang, and Ziwei Liu. Venhancer: Generative space-time enhancement for video generation. *arXiv preprint arXiv:2407.07667*, 2024. 3, 6, 14
- [13] Jonathan Ho and Tim Salimans. Classifier-free diffusion guidance. *arXiv preprint arXiv:2207.12598*, 2022. 12
- [14] Jonathan Ho, Ajay Jain, and Pieter Abbeel. Denoising diffusion probabilistic models. *Advances in neural information processing systems*, 33:6840–6851, 2020. 2
- [15] Jonathan Ho, Tim Salimans, Alexey Gritsenko, William Chan, Mohammad Norouzi, and David J Fleet. Video diffusion models. *Advances in Neural Information Processing Systems*, 35:8633–8646, 2022. 5
- [16] Mengshun Hu, Kui Jiang, Zheng Wang, Xiang Bai, and Ruimin Hu. Cycmunet+: Cycle-projected mutual learning for spatial-temporal video super-resolution. *IEEE Transactions on Pattern Analysis and Machine Intelligence*, 2023. 3
- [17] Ziqi Huang, Yinan He, Jiashuo Yu, Fan Zhang, Chenyang Si, Yuming Jiang, Yuanhan Zhang, Tianxing Wu, Qingyang Jin, Nattapol Chanpaisit, et al. Vbench: Comprehensive benchmark suite for video generative models. In *Proceedings of the IEEE/CVF Conference on Computer Vision and Pattern Recognition*, pages 21807–21818, 2024. 6
- [18] Phillip Isola, Jun-Yan Zhu, Tinghui Zhou, and Alexei A Efros. Image-to-image translation with conditional adversarial networks. In *Proceedings of the IEEE conference on computer vision and pattern recognition*, pages 1125–1134, 2017. 4
- [19] Junjie Ke, Qifei Wang, Yilin Wang, Peyman Milanfar, and Feng Yang. Musiq: Multi-scale image quality transformer. In *Proceedings of the IEEE/CVF international conference on computer vision*, pages 5148–5157, 2021. 6
- [20] Diederik P Kingma. Adam: A method for stochastic optimization. *arXiv preprint arXiv:1412.6980*, 2014. 6
- [21] Wei-Sheng Lai, Jia-Bin Huang, Oliver Wang, Eli Shechtman, Ersin Yumer, and Ming-Hsuan Yang. Learning blind video temporal consistency. In *Proceedings of the European conference on computer vision (ECCV)*, pages 170–185, 2018. 6
- [22] Jingyun Liang, Jiezhong Cao, Guolei Sun, Kai Zhang, Luc Van Gool, and Radu Timofte. Swinir: Image restoration using swin transformer. In *Proceedings of the IEEE/CVF International Conference on Computer Vision (ICCV) Workshops*, pages 1833–1844, 2021. 3
- [23] Jingyun Liang, Yuchen Fan, Xiaoyu Xiang, Rakesh Ranjan, Eddy Ilg, Simon Green, Jiezhong Cao, Kai Zhang, Radu Timofte, and Luc V Gool. Recurrent video restoration transformer with guided deformable attention. *Advances in Neural Information Processing Systems*, 35:378–393, 2022. 2, 3
- [24] Jingyun Liang, Jiezhong Cao, Yuchen Fan, Kai Zhang, Rakesh Ranjan, Yawei Li, Radu Timofte, and Luc Van Gool. Vrt: A video restoration transformer. *IEEE Transactions on Image Processing*, 2024. 3
- [25] Xinqi Lin, Jingwen He, Ziyang Chen, Zhaoyang Lyu, Bo Dai, Fanghua Yu, Wanli Ouyang, Yu Qiao, and Chao Dong. Diff-

- bir: Towards blind image restoration with generative diffusion prior. *arXiv preprint arXiv:2308.15070*, 2023. 3, 6, 14
- [26] Chengxu Liu, Huan Yang, Jianlong Fu, and Xueming Qian. Learning trajectory-aware transformer for video super-resolution. In *Proceedings of the IEEE/CVF conference on computer vision and pattern recognition*, pages 5687–5696, 2022. 3
- [27] Hongying Liu, Zubo Ruan, Peng Zhao, Chao Dong, Fanhua Shang, Yuanyuan Liu, Linlin Yang, and Radu Timofte. Video super-resolution based on deep learning: a comprehensive survey. *Artificial Intelligence Review*, 55(8):5981–6035, 2022. 3
- [28] Yihao Liu, Hengyuan Zhao, Kelvin CK Chan, Xintao Wang, Chen Change Loy, Yu Qiao, and Chao Dong. Temporally consistent video colorization with deep feature propagation and self-regularization learning. *Computational Visual Media*, 10(2):375–395, 2024. 12
- [29] Chao Ma, Chih-Yuan Yang, Xiaokang Yang, and Ming-Hsuan Yang. Learning a no-reference quality metric for single-image super-resolution. *Computer Vision and Image Understanding*, 158:1–16, 2017. 6
- [30] Seungjun Nah, Sungyong Baik, Seokil Hong, Gyeongsik Moon, Sanghyun Son, Radu Timofte, and Kyoung Mu Lee. Ntire 2019 challenge on video deblurring and super-resolution: Dataset and study. In *Proceedings of the IEEE/CVF conference on computer vision and pattern recognition workshops*, pages 0–0, 2019. 5
- [31] Kepan Nan, Rui Xie, Penghao Zhou, Tiehan Fan, Zhenheng Yang, Zhijie Chen, Xiang Li, Jian Yang, and Ying Tai. Openvid-1m: A large-scale high-quality dataset for text-to-video generation. *arXiv preprint arXiv:2407.02371*, 2024. 5
- [32] Robin Rombach, Andreas Blattmann, Dominik Lorenz, Patrick Esser, and Björn Ommer. High-resolution image synthesis with latent diffusion models. In *Proceedings of the IEEE/CVF conference on computer vision and pattern recognition*, pages 10684–10695, 2022. 2
- [33] Tim Salimans and Jonathan Ho. Progressive distillation for fast sampling of diffusion models. *arXiv preprint arXiv:2202.00512*, 2022. 3
- [34] Xin Tao, Hongyun Gao, Renjie Liao, Jue Wang, and Jiaya Jia. Detail-revealing deep video super-resolution. In *Proceedings of the IEEE international conference on computer vision*, pages 4472–4480, 2017. 5
- [35] InternLM Team. Internlm-xcomposer2: A vision-language large model for advanced text-image comprehension and composition. <https://huggingface.co/internlm/internlm-xcomposer2-v1-7b>, 2024. 3
- [36] Yapeng Tian, Yulun Zhang, Yun Fu, and Chenliang Xu. Tdan: Temporally-deformable alignment network for video super-resolution. In *Proceedings of the IEEE/CVF conference on computer vision and pattern recognition*, pages 3360–3369, 2020. 3
- [37] Jianyi Wang, Kelvin CK Chan, and Chen Change Loy. Exploring clip for assessing the look and feel of images. In *Proceedings of the AAAI Conference on Artificial Intelligence*, pages 2555–2563, 2023. 6
- [38] Jianyi Wang, Zongsheng Yue, Shangchen Zhou, Kelvin CK Chan, and Chen Change Loy. Exploiting diffusion prior for real-world image super-resolution. *International Journal of Computer Vision*, pages 1–21, 2024. 3
- [39] Ruohao Wang, Xiaohui Liu, Zhilu Zhang, Xiaohe Wu, Chunmei Feng, Lei Zhang, and Wangmeng Zuo. Benchmark dataset and effective inter-frame alignment for real-world video super-resolution. In *Proceedings of the IEEE/CVF conference on computer vision and pattern recognition*, pages 1168–1177, 2023. 5
- [40] Ting-Chun Wang, Ming-Yu Liu, Jun-Yan Zhu, Guilin Liu, Andrew Tao, Jan Kautz, and Bryan Catanzaro. Video-to-video synthesis. *arXiv preprint arXiv:1808.06601*, 2018. 4
- [41] Xintao Wang, Ke Yu, Shixiang Wu, Jinjin Gu, Yihao Liu, Chao Dong, Yu Qiao, and Chen Change Loy. ESRGAN: Enhanced super-resolution generative adversarial networks. In *Proceedings of the European Conference on Computer Vision (ECCV) Workshops*, 2018. 3
- [42] Xintao Wang, Kelvin CK Chan, Ke Yu, Chao Dong, and Chen Change Loy. EDVR: Video restoration with enhanced deformable convolutional networks. In *Proceedings of the IEEE/CVF conference on computer vision and pattern recognition workshops*, pages 0–0, 2019. 2, 3
- [43] Xintao Wang, Liangbin Xie, Chao Dong, and Ying Shan. Real-ESRGAN: Training real-world blind super-resolution with pure synthetic data. In *Proceedings of the IEEE/CVF international conference on computer vision*, pages 1905–1914, 2021. 3, 5, 6, 14
- [44] Yingwei Wang, Takashi Isobe, Xu Jia, Xin Tao, Huchuan Lu, and Yu-Wing Tai. Compression-aware video super-resolution. In *Proceedings of the IEEE/CVF Conference on Computer Vision and Pattern Recognition (CVPR)*, pages 2012–2021, 2023. 3
- [45] Haoning Wu, Erli Zhang, Liang Liao, Chaofeng Chen, Jingwen Hou, Annan Wang, Wenxiu Sun, Qiong Yan, and Weisi Lin. Exploring video quality assessment on user generated contents from aesthetic and technical perspectives. In *Proceedings of the IEEE/CVF International Conference on Computer Vision*, pages 20144–20154, 2023. 6
- [46] Jay Zhangjie Wu, Yixiao Ge, Xintao Wang, Stan Weixian Lei, Yuchao Gu, Yufei Shi, Wynne Hsu, Ying Shan, Xiaohu Qie, and Mike Zheng Shou. Tune-a-video: One-shot tuning of image diffusion models for text-to-video generation. In *Proceedings of the IEEE/CVF International Conference on Computer Vision*, pages 7623–7633, 2023. 5
- [47] Bin Xia, Yulun Zhang, Shiyin Wang, Yitong Wang, Xinglong Wu, Yapeng Tian, Wenming Yang, and Luc Van Gool. DiffIR: Efficient diffusion model for image restoration. In *Proceedings of the IEEE/CVF International Conference on Computer Vision*, pages 13095–13105, 2023. 3
- [48] Xi Yang, Chenhang He, Jianqi Ma, and Lei Zhang. Motion-guided latent diffusion for temporally consistent real-world video super-resolution. In *European Conference on Computer Vision*, pages 224–242. Springer, 2025. 3, 6, 12, 14
- [49] Peng Yi, Zhongyuan Wang, Kui Jiang, Junjun Jiang, and Jiayi Ma. Progressive fusion video super-resolution network via exploiting non-local spatio-temporal correlations. In

- IEEE International Conference on Computer Vision (ICCV)*, pages 3106–3115, 2019. [5](#)
- [50] Kai Zhang, Jingyun Liang, Luc Van Gool, and Radu Timofte. Designing a practical degradation model for deep blind image super-resolution. In *Proceedings of the IEEE/CVF International Conference on Computer Vision (ICCV)*, pages 4791–4800, 2021. [3](#)
- [51] Lvmin Zhang, Anyi Rao, and Maneesh Agrawala. Adding conditional control to text-to-image diffusion models, 2023. [3](#)
- [52] Richard Zhang, Phillip Isola, Alexei A Efros, Eli Shechtman, and Oliver Wang. The unreasonable effectiveness of deep features as a perceptual metric. In *Proceedings of the IEEE conference on computer vision and pattern recognition*, pages 586–595, 2018. [4](#)
- [53] Shangchen Zhou, Peiqing Yang, Jianyi Wang, Yihang Luo, and Chen Change Loy. Upscale-a-video: Temporal-consistent diffusion model for real-world video super-resolution. In *Proceedings of the IEEE/CVF Conference on Computer Vision and Pattern Recognition*, pages 2535–2545, 2024. [3](#), [5](#), [6](#), [12](#), [14](#)

Appendix

A. More Ablation Studies

A.1. Effectiveness of Progressive Learning Strategy

To validate the effectiveness of the Progressive Learning Strategy, we conduct ablation studies on different training approaches, as illustrated in Fig. 8. We compare three strategies: (1) Direct Learning Strategy: The model is trained on all degradation levels directly, with only the temporal layers tuned. This strategy is commonly used in previous works [48, 53]. (2) 2-Stage Learning Strategy: The model is initially trained on simple degradations with only temporal layers tuned. Subsequently, training continues with more complex degradations, unlocking all parameters. (3) Proposed Progressive Learning Strategy: Training begins on simple degradations with only temporal layers tuned. Complex degradations are then introduced to refine the model’s capabilities, and in the final stage, all parameters are fine-tuned using high-quality data.

We evaluate these strategies on 10 videos from the YouHQ dataset. As shown in Table 5, the Progressive Learning Strategy significantly outperforms the other approaches, particularly in restoration quality and temporal consistency. These results highlight the importance of a well-structured progressive training scheme in adapting the model incrementally to complex video restoration tasks, ensuring both stability and superior performance.

Exp.	PSNR \uparrow	CLIP-IQA \uparrow	MUSIQ \uparrow	DOVER \uparrow	$E_{warp}^*\downarrow$
(1)	23.299	0.8432	68.182	0.864	2.582
(2)	23.591	0.8383	68.449	0.866	2.236
(3)	24.172	0.8666	68.982	0.870	1.707

Table 5. Ablation study of different training strategies. The results demonstrate that our Progressive Learning Strategy (PLS) consistently improve the performance across both quality and temporal consistency metrics.

A.2. Effectiveness of Text Prompts

Our model supports both text-guided and text-free restoration approaches. As shown in Fig. 9, incorporating classifier-free guidance [13] with meaningful text prompts significantly enhances visual quality compared to using empty prompts. This improvement is particularly evident in fine-grained details, such as the enhanced fur textures of the piglet and owl, sharper vegetation in the zebra scene, and more distinct zebra patterns in distant regions. These results demonstrate that appropriate text prompts can effectively guide the restoration process, enhancing intricate textures while maintaining a natural and realistic appearance.

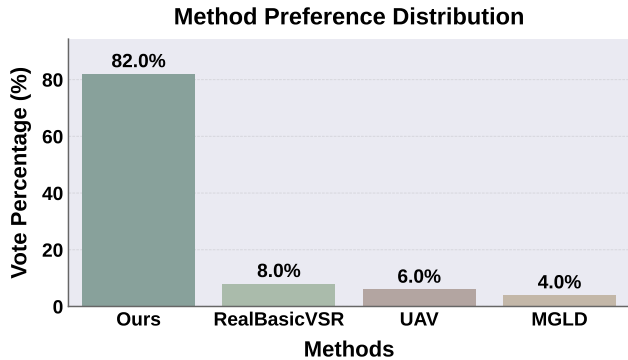


Figure 7. Quantitative comparison of user preferences among different video restoration methods. Our method achieves the highest preference rate (82.0%) in the user study, significantly outperforming RealBasicVSR [9], MGLD [48], and UAV [53].

The ability of text prompts to improve results highlights their role in activating the pretrained generative priors, enabling the model to leverage its full potential. These findings align with prior work [53], further validating that text guidance is a valuable tool for boosting the performance of large-scale generative models in restoration tasks.

B. User Study

We conducted a user study to evaluate perceptual quality through blind comparison. Twenty participants with a computer vision background were asked to compare restoration results from RealBasicVSR [9], MGLD [48], UAV [53], and our method. The study included 20 test sets, containing both real-world and synthetic degraded videos. Participants were instructed to select the most visually appealing result based on three criteria: overall fidelity, detail preservation, and temporal consistency. To ensure unbiased evaluations, method names were hidden, and display order was randomized. As shown in Fig. 7, our method achieved the highest preference rate across various degradation scenarios, demonstrating its superior perceptual quality in restoration tasks.

C. Trade-off Between Visual Quality and Temporal Consistency

In video restoration tasks, achieving a balance between visual quality and temporal consistency is a well-known challenge [28, 48, 53], akin to the perception-distortion trade-off in image restoration [4]. Higher restoration quality typically enhances texture detail but can often lead to reduced temporal consistency across frames.

To illustrate this trade-off, we analyze MUSIQ (video quality) and Warping Error (temporal consistency) scores on the YouHQ40 dataset, as shown in Fig. 10. The ideal

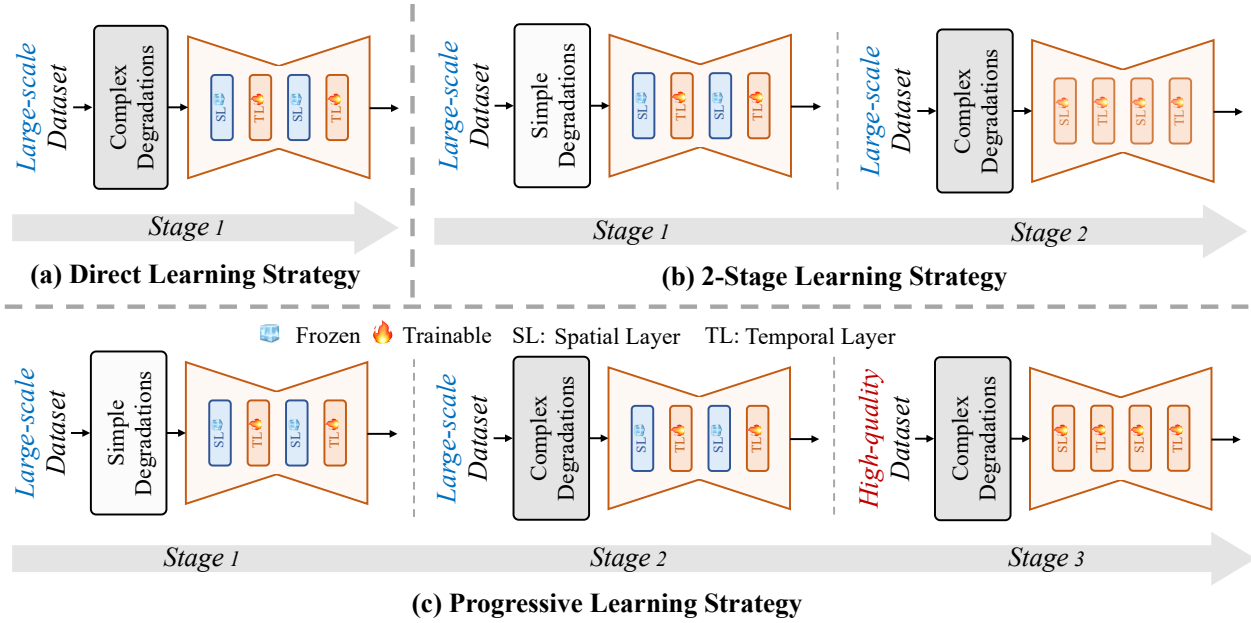


Figure 8. Illustration of three training strategy variants: Direct Learning Strategy, 2-Stage Learning Strategy, and Progressive Learning Strategy. The proposed Progressive Learning Strategy can not only stabilize the training procedure but also improve performance.

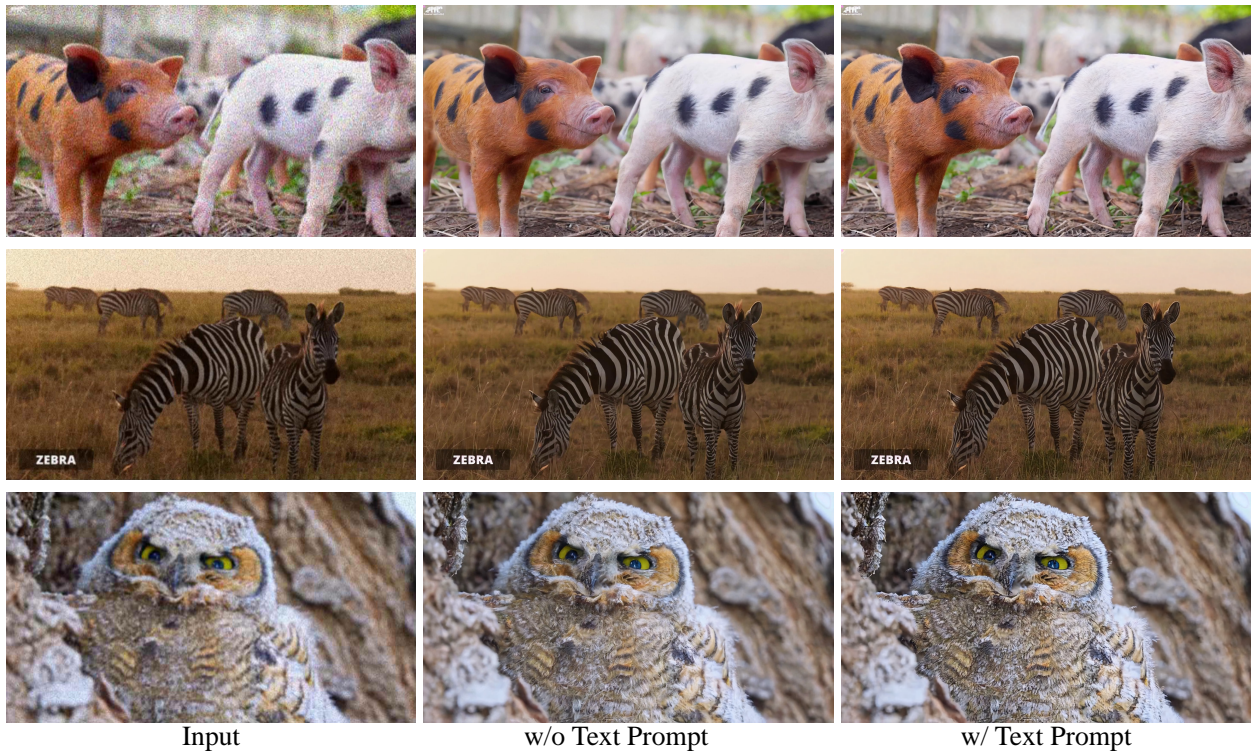


Figure 9. Visual comparison of restoration results with and without text prompts. Incorporating meaningful text prompts as guidance significantly enhances visual quality, improving texture sharpness, fine-grained details, and overall realism. **(Zoom-in for best view)**

performance lies in the lower-right region, reflecting high video quality and low warping error. As observed, image-

based methods achieve higher quality scores but poor temporal consistency, while video-based approaches maintain

Datasets	Metrics	Real-ESRGAN[43]	SD ×4 Upscaler[1]	DiffBIR[25]	RealBasicVSR[9]	MGLD[48]	VEnhancer[12]	UAV[53]	Ours
VideoLQ	NRQM↑	5.772	4.956	6.430	6.175	5.990	4.351	5.090	6.257
	CLIP-IQA↑	0.633	0.682	0.611	0.669	0.698	0.659	0.639	0.682
	MUSIQ↑	49.837	34.864	53.575	55.975	47.958	43.555	36.369	57.812
	DOVER↑	0.728	0.518	0.679	0.742	0.730	0.657	0.632	0.747

Table 6. Quantitative comparison with state-of-the-art methods on VideoLQ dataset.

better temporal coherence at the cost of reduced quality. Our method achieves a favorable balance between these competing objectives, demonstrating effectiveness in mitigating the inherent trade-offs in video restoration tasks.

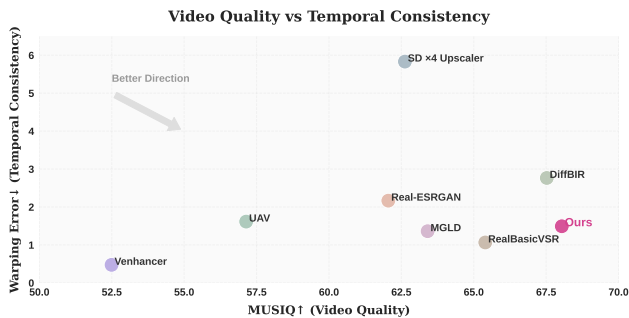


Figure 10. Analysis of the trade-off between video quality (MUSIQ) and temporal consistency (Warping Error) on YouHQ40 dataset. Methods towards the lower-right corner achieve better overall performance, with higher MUSIQ and lower warping error.

D. More Quantitative and Qualitative Comparisons

D.1. More Quantitative Evaluation

We provide additional quantitative evaluations on the VideoLQ [9] dataset, which contains real-world low-quality videos with diverse degradation types. As shown in Table 6, our method consistently outperforms existing approaches across all metrics. Notably, we achieve significant improvements in perceptual quality metrics, with the highest scores in MUSIQ (57.812). The superior DOVER score (0.747) further validates our method’s effectiveness in maintaining both visual quality and temporal consistency. These results align with our findings in the main paper, demonstrating our method’s robust performance across different real-world scenarios.

D.2. More Qualitative Results

We conduct comprehensive visual comparisons against state-of-the-art approaches, including both image-based methods (ESRGAN [43], SD ×4 Upscaler [1], DiffBIR [25]) and video-based methods (RealBasicVSR [9], MGLD [48], VEnhancer [12], UAV [53]). Figs. 12 and 11

showcase the qualitative results on synthetic and real-world test videos, respectively. Our method demonstrates superior capability in recovering diverse textures and structures across various scenarios, including architectural elements (wall textures, brick patterns), organic details (facial features, hair strands), natural scenes (vegetation, marine life), and high-frequency patterns (text, dental structures). The restored results exhibit both high fidelity to reference images and rich textural details, while avoiding common artifacts like over-smoothing or false pattern generation.

E. Video Demo

We also provide a demonstration video [DiffVSR.mp4] to showcase the capabilities of our method on both synthetic and real-world videos. The video highlights temporal coherence and dynamic detail preservation, which are better appreciated in motion than through static comparisons. **The demonstration video is included in the supplementary materials. Note that due to file size limitations, the video has been compressed; the original results exhibit even higher visual quality.**

F. Limitations

While DiffVSR achieves significant improvements over existing methods, it has several limitations: (1) As a diffusion-based model, DiffVSR requires repetitive iterations for inference, resulting in slower processing times. This makes it challenging to deploy in real-time applications. (2) DiffVSR struggles with certain challenging scenarios, such as small faces, small human bodies, and complex street scenes, due to inherited limitations of current diffusion-based generative models. Addressing these issues may require additional task-specific adaptations. (3) Due to limited computational resources, we have not conducted larger-scale experiments with increased input sizes or batch sizes. Scaling up the training process with more GPUs could further improve DiffVSR’s performance.

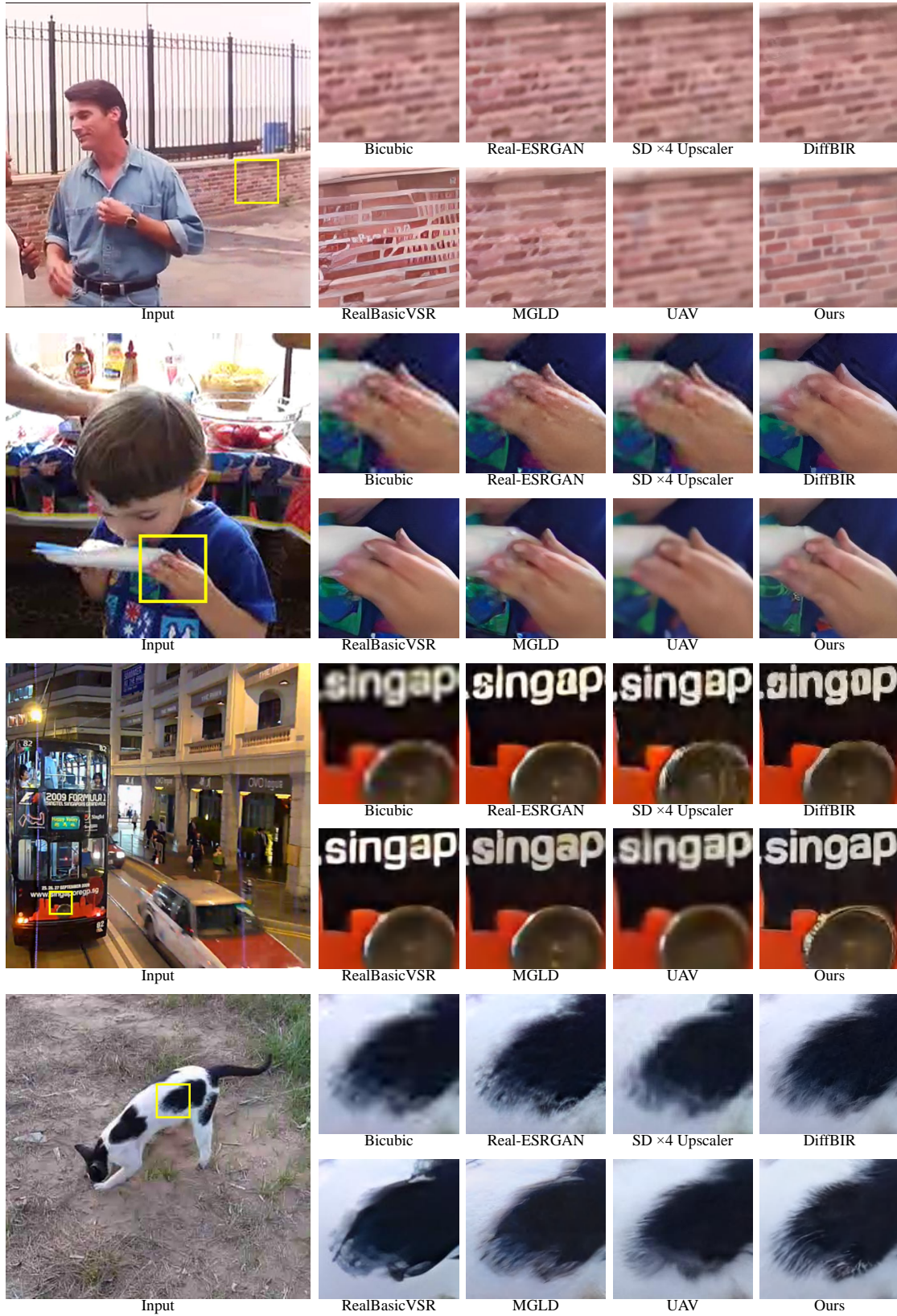


Figure 11. Qualitative comparisons on real-world videos. Our method effectively recovers fine details while maintaining natural textures. **(Zoom-in for best view)**

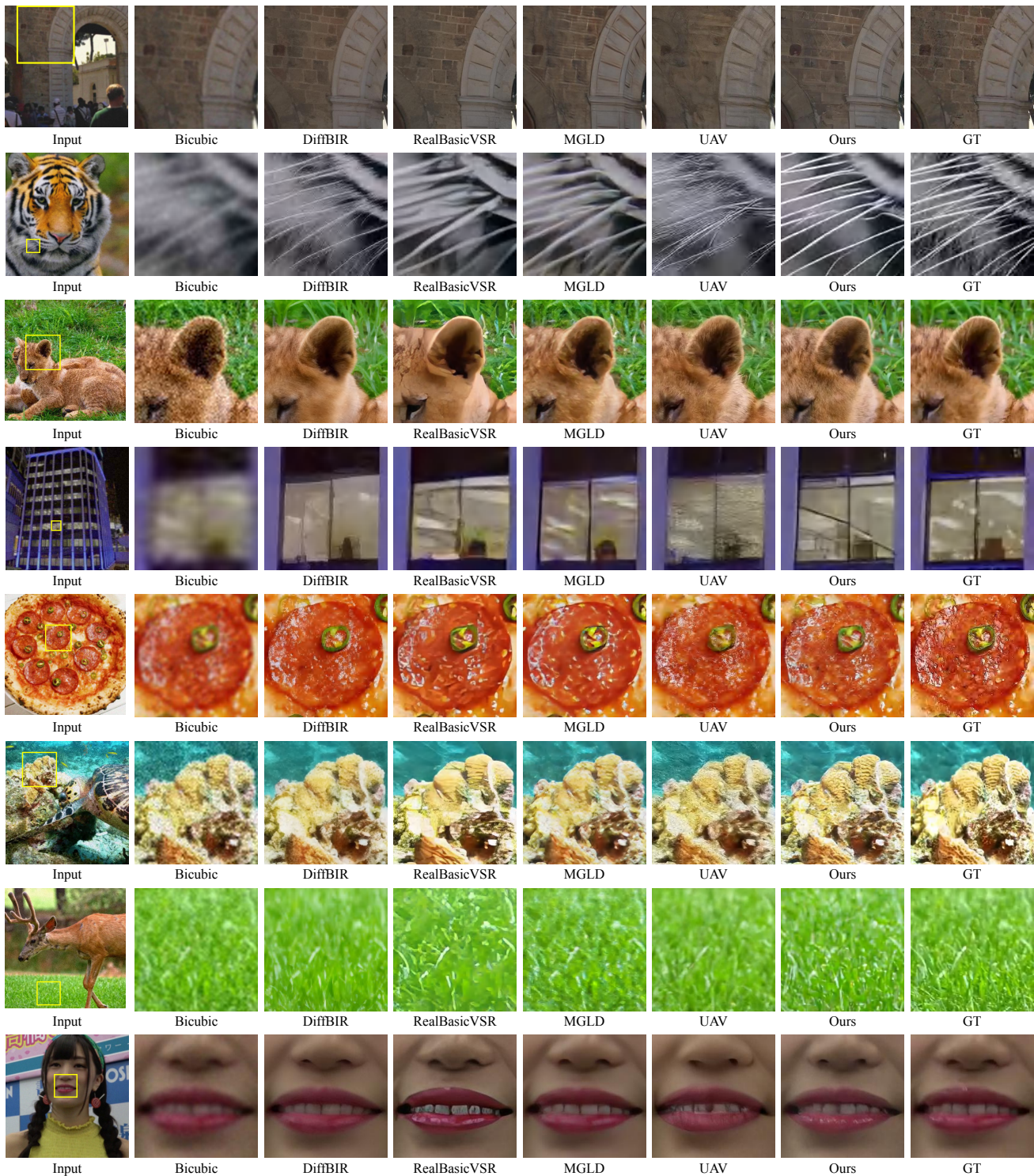


Figure 12. Qualitative comparisons on synthetic datasets. Our method demonstrates superior capability in recovering accurate facial details and textual information, while other methods struggle with either over-smoothing or detail distortion. **(Zoom-in for best view)**